

Picosecond Dynamics of CN^- -Ligated Ferric Cytochrome c after Photoexcitation Using Time-resolved Vibrational Spectroscopy

Jooyoung Kim, Jaeheung Park, Salina A Chowdhury, and Manho Lim*

Department of Chemistry and Chemistry Institute of Functional Materials, Pusan National University, Busan 609-735 Korea

*E-mail: mhlum@pusan.ac.kr

Received October 29, 2010, Accepted November 11, 2010

The dynamics of the CN^- -ligated ferric cytochrome c (CytcCN) in D_2O at 283 K following Q-band photoexcitation at 575 nm was observed using femtosecond time-resolved vibrational spectroscopy. The equilibrium vibrational spectrum of the CN stretching mode of CytcCN shows two overlapping bands: one main band (82%) at 2122 cm^{-1} with 23 cm^{-1} full width at half maximum (fwhm) and the other band (18%) at 2116 cm^{-1} with 7 cm^{-1} fwhm. The time-resolved spectra show bleaching of the CN fundamental mode of CytcCN and two absorption features at lower energies. The bleach signal and both absorption features are all formed within the time resolution of the experiment ($< 200\text{ fs}$) and decay with a life time of 1.9 ps. One transient absorption feature, appearing immediately red to the bleach signal, results from the thermal excitation of low-frequency modes of the heme that anharmonically couple to the CN fundamental mode, thereby shifting the CN mode to lower energies. The shift of the CN mode decays with a lifetime of 2 ps, equivalent to the time scale for vibrational cooling of the low-frequency heme modes. The other transient absorption feature, which is 3.3 times weaker than the bleach signal and shifted 27 cm^{-1} toward lower energies, is attributed to the CN mode in an electronically excited state where the CN bond is weakened with a lowered extinction coefficient. These observations suggest that photoexcited CytcCN mainly undergoes ultrafast radiationless relaxation, causing photo-deligation of CN^- from CytcCN highly inefficient. As also observed in CN^- -ligated myoglobin, inefficient ligand photodissociation might be a general property of CN^- -ligated ferric hemes.

Key Words: CN^- -Ligated cytochrome c, Femtosecond vibrational spectroscopy, Ferric cytochrome c, Picosecond dynamics, Q-band photoexcitation

Introduction

Detailed knowledge of the dynamical and structural properties of proteins is essential to a full understanding of protein function. Heme proteins, such as hemoglobin (Hb), myoglobin (Mb), and cytochrome c (Cytc) have been served as model systems in studying protein dynamics and structure.¹⁻⁴ The binding of a small ligand to heme proteins has been greatly studied in order to understand the relationships between protein structure, dynamics, and function.^{2,3,5-14} In particular, the rebinding dynamics of a number of neutral diatomic molecules, such as CO, NO, or O_2 to ferrous heme or heme proteins has been widely investigated both experimentally and theoretically. By contrast, only a few experiments have been carried out on the rebinding dynamics of ionic molecules to heme proteins.¹⁵

CN^- is an ionic ligand that binds strongly to ferric heme and heme proteins.¹⁶⁻²¹ Since a charged ligand can form a strong hydrogen bond, which can influence the spectroscopic and structural characteristics of the active site, CN^- can serve as a good probe for the environments of the active site of a protein.²²⁻²⁴ Since CN^- is isoelectronic to CO with negative charge, its rebinding characteristics can be well compared with that of CO, the most studied ligand.

Recently, the dynamics of photoexcited CN^- bound ferric Mb (MbCN) was investigated after Soret band excitation at 405 nm using both time-resolved electronic spectroscopy and vibrational spectroscopy.¹⁵ A transient absorption signal in the 360-390 nm range showed ultrafast decay with a time constant of 3.6 ps. The transient vibrational spectra showed instantaneous

bleaching of the CN stretch fundamental of MbCN and the appearance of a five-times weaker, red-shifted transient absorption band that decayed with a 3-4 ps time constant. Two possible assignments were proposed for the new red-shifted absorption band: the CN fundamental in the electronically excited state of MbCN or the vibrationally excited state of CN in the ground electronic state of the heme. Assignment of the new absorption band to the vibrationally excited state of CN requires ultrafast vibrational relaxation time of less than 1 ps from the $\nu = 1$ state, which is populated by the rebinding of the dissociated ligand with a 3-4 ps time constant. For assignment of the new band to the CN fundamental in the electronically excited state of MbCN, the CN bond ought to be weakened in the electronically excited state to explain the red-shifted absorption. To be consistent with the five-times weaker absorption, the extinction coefficient of the new band is also lowered by an equal amount. More recently, using nonequilibrium molecular dynamics simulation, Meuwly and coworkers found that the vibrationally excited state of the CN stretching mode of MbCN relaxes on a time scale of hundreds of picoseconds, which enabled them to exclude the vibrationally excited state of CN in the ground electronic state of the heme as a candidate for assignment of the new absorption observed in time-resolved vibrational spectroscopy.^{25,26} Instead, they suggested that the new absorption arises from the electronically excited state with a weakened CN bond and, thus, photodissociation of CN^- from MbCN after Soret band excitation is unlikely. This can be contrasted with photodissociation of CN^- from cyanide-bound ferrous Mb and homodimeric Hb.²⁰ Considering the fact that many ligands such as

CO, NO, and O₂ undergo ultrafast and efficient photodissociation from heme, negligible ligand photodissociation from MbCN requires further investigation. A comparative study of various heme proteins would be useful to determine whether the reported photo-inertness of MbCN is a general feature of CN⁻-bound ferric heme.

Cytochrome c is a ubiquitous small electron transfer protein with one heme cofactor. The heme iron of Cytc is hexacoordinated with two axial ligands, His18 and Met80.²⁷ The distal axial ligand, Met80, readily dissociates in ferric Cytc and can be displaced by internal residues or by exogenous ligands such as imidazole, pyridine, and various anions – including CN⁻, F⁻, N₃⁻, and SCN⁻.²⁸⁻³⁰ Oxidation state of Fe in the heme plays an important role in the photodissociation of Met80. Whereas Met80 is instantaneously photolyzed and geminately rebinds with time constants of 5 and 10 ps in ferrous Cytc, it is not photolabile in ferric Cytc.¹³ For ferric Cytc, the photoexcited state relaxes mainly by vibrational cooling in the ground electronic state of the heme.¹³ However, CN⁻ strongly binds to ferric Cytc and displaces the internal ligand Met80.^{16,17} Since there is a displaced Met80 and no distal histidine, the distal environment of CytcCN is quite different from that of Mb. Therefore, study of CytcCN will reveal the influence of the distal environment on heme photodynamics and ligand photodissociation.

Here we measured the dynamics of photoexcited CytcCN in D₂O at 283 K using femtosecond vibrational spectroscopy. After Q-band excitation at 575 nm, bleaching of the CN fundamental and a 27 cm⁻¹ red-shifted new absorption appear instantaneously. The dynamics of the bleach signal and the new absorption is similar to that in MbCN after Soret band excitation. The photodynamics of CytcCN after Q-band excitation is interpreted by comparing with that of MbCN.

Materials and Methods

The time-resolved vibrational spectrometer used here is described in detail elsewhere.^{3,9,31} Two optical parametric amplifiers (OPA) were used to generate a pump pulse at 575 nm with 3 μJ of energy and a tunable mid-IR probe pulse.³² The polarization of the probe pulse was set parallel or perpendicular to that the pump pulse to obtain the desired polarized absorbance spectra. The isotropic spectrum was also measured by setting the magic angle (54.7°) between the polarizations of two pulses. A spectral resolution of *ca.* 1.7 cm⁻¹/pixel at 2120 cm⁻¹ was achieved using a 64-elements N₂(*l*)-cooled HgCdTe array detector and a 320 mm monochromator with a 150 l/mm grating. The pump-induced absorbance change, Δ*A* was obtained by chopping the pump pulse to half the repetition frequency of the laser. High sensitivity in Δ*A* (less than 1 × 10⁻⁴ rms) was routinely achieved by maintaining the excellent stability of the IR light source (< 0.5% rms). The instrument response function was typically 180 fs.

A 20 mM CytcCN solution was prepared by dissolving horse heart cytochrome c (Sigma) in 0.2 M potassium phosphate buffer (pD 7.4)³³ and then adding a three-fold excess of KCN. The formation of CytcCN was confirmed by UV-vis and IR spectroscopy. The sample was loaded in a gastight 50-μm-path-length rotating sample cell with two 2-mm-thick CaF₂ windows. The

integrity and concentration of the sample were confirmed throughout the experiments using both UV-vis and IR spectroscopy. The sample cell was rotated fast enough to maintain a fresh volume of the sample for each photoexciting laser pulse during data collection. The temperature of the sample cell was maintained at 283 ± 1 K using a circulating bath connected to the sample cell block. Deuterated water (D₂O) was used as the solvent to ensure the sample was transmitting sufficiently in the interested spectral region, 2050 - 2200 cm⁻¹.

Results and Discussion

Figure 1(a) shows the equilibrium vibrational spectrum of the CN stretching mode of CytcCN in the deuterated phosphate buffer solution. The CN fundamental mode in CytcCN consists of two overlapping bands, which is well modeled by two Gaussian functions: one main band (82%) at 2122 cm⁻¹ with a 23 cm⁻¹ full width at half maximum (fwhm) and the other (18%) at 2116 cm⁻¹ with a 7 cm⁻¹ fwhm. It is well known that vibrational bands arise from different conformations of a protein.⁵ Two vibrational bands suggest that CytcCN has at least two conformations. The main band in CytcCN is located at a position that is similar to those in MbCN (2125 - 2126 cm⁻¹) and in CN⁻-ligated ferric microperoxidase (MpCN; 2124.2 cm⁻¹), but its bandwidth is much broader than those in MbCN (9 - 13.3 cm⁻¹) and in MpCN (8.6 cm⁻¹).^{15,19} The width of the main band in CytcCN suggests that the distal environments of the main conformation of CytcCN are much more heterogeneous than in MbCN, which has a distal histidine, and the solvent surroundings of MpCN. The smaller band at 2116 cm⁻¹ is much more red-shifted and narrower than those in MbCN and MpCN. The smaller band clearly reflects the unique environment of the active site in some fraction (18%) of CytcCN. Since the CN fundamental mode of CytcCN has two bands, its integrated extinction coefficient was calculated to compare its intensity with the CN mode of other heme systems that have a single band. The integrated extinction coefficient of the CN fundamental in CytcCN was calculated to be 1200 M⁻¹cm⁻² using the protein concentration obtained from the visible absorption of our sample (ε = 9200 M⁻¹cm⁻¹ at 450 nm).¹⁷ This value is similar to that reported for MbCN by Helbing *et al* (720 - 1200 M⁻¹cm⁻²) but about three-times smaller than that reported by Reddy *et al* (3300 M⁻¹cm⁻²).^{15,19} Under our sample condition of deuterated buffer at pD 7.4, most of the excess CN⁻ not bound to the protein exists in the form of DCN, the fundamental of which is located at 1887 cm⁻¹.^{15,34} No CN fundamentals from CN⁻ (2079 cm⁻¹) and HCN (2093 cm⁻¹)¹⁵ were observed in the IR absorption spectrum of our sample.

Figure 1(b) shows the time-resolved vibrational spectra near the CN fundamental of CytcCN after photoexcitation of the protein in D₂O at 283 K using a pump pulse at 575 nm. Upon excitation of the Q-band of CytcCN, the transient infrared spectra show a strong bleach signal near 2120 cm⁻¹ and smaller absorption feature to the red of the bleach signal. Both the bleach and the absorption feature form in less than 200 fs, our instrumental response function, and decay with a picosecond time scale. The bleach signal arises from the reduction in the population of the CN stretch fundamental vibration. As can be seen

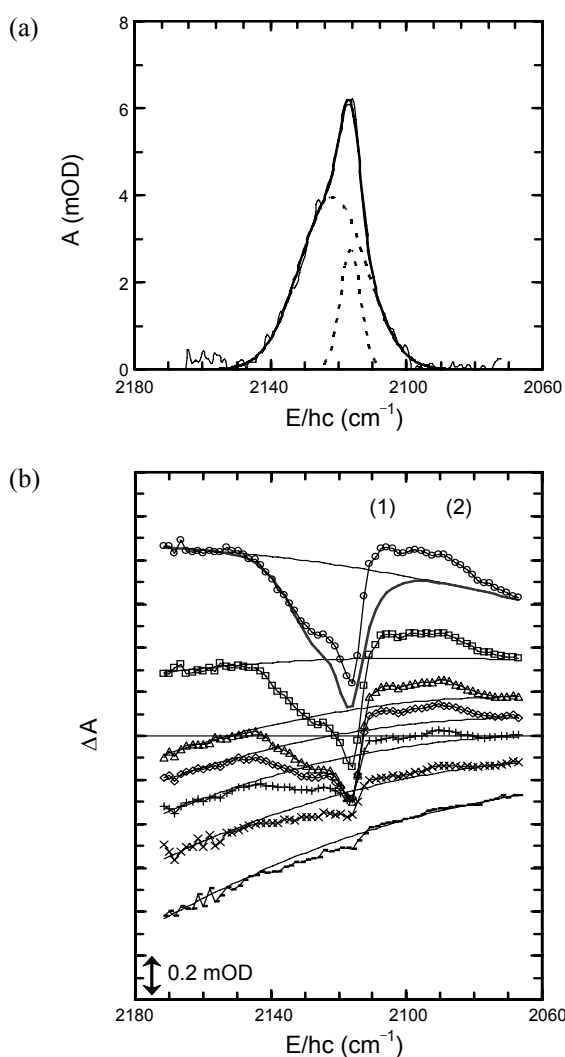


Figure 1. (a) Equilibrium vibrational spectrum of CytCN in D_2O in the region of the CN stretching band. The band (thin solid line) is well fit with a sum of two Gaussians (thick solid line). Two Gaussian components are also shown (dotted lines). The background absorption from the solvent was subtracted from data for clarity. (b) Representative time-resolved vibrational spectra near the CN stretching band following excitation of CytCN in D_2O at 283 K (symbols) using a pump pulse at 575 nm. The unit of the ordinate is the difference in optical density (OD; 1 mOD = 10^{-3} OD). Pump-probe delays are 0.3, 0.56, 1, 1.8, 3.2, 5.6, and 10 ps from top to bottom. Spectrum was modeled with one bleach plus two absorption features with a quadratic polynomial (thin solid line). The quadratic polynomial represents the background signal arising from the cross-phase modulation between the overlapping pump and probe pulses and thermal change in the solvent spectrum (see text). For comparison, the CN stretching band of CytCN in the equilibrium spectrum is inverted, scaled, and overlapped with time-resolved spectrum at 0.3 ps by sharing the same background signal (thick solid line).

in Figure 1(b), the smaller absorption consists of two absorption features: one immediately to the red of the CN fundamental and the other red-shifted by *ca.* 27 cm^{-1} . As has been done in MbCN, we labeled them 1 and 2, respectively (see Figure 1(b)).¹⁵ Band 2, initially centered at 2090 cm^{-1} , is approximately three-times weaker than the bleach signal. Transient spectra also reveal a significant change in the offset, which arises from an

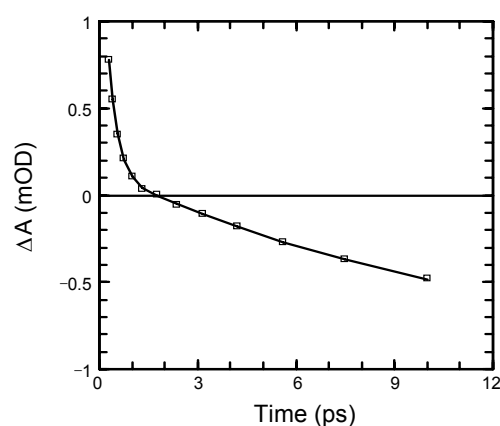


Figure 2. The time-dependent change of the background signal in the transient. The value is the constant term of the quadratic polynomial fitting the background. The kinetics is well described by a biexponential function, $0.66 \exp(-t/0.3\text{ ps}) + 0.34 \exp(-t/13\text{ ps})$.

evolving broad background. This has been attributed to cross-phase modulation between overlapping pump and probe pulses as well as the spectral change of the solvent resulting from the thermal relaxation of the protein. The kinetics of the background offset (the constant term in the quadratic polynomial fitting the background), plotted in Figure 2, is well described by a biexponential function, $0.66 \exp(-t/0.3\text{ ps}) + 0.34 \exp(-t/13\text{ ps})$. The fast decay (0.3 ps) is related to the instrument response function and the slow decay is related to the time for the transfer of thermal energy from the protein to the solvent. A thermal transfer time of 13 ps is consistent with the reported time of 5 - 10 ps in MbCN.¹⁵

The transient spectra shown in Figure 1(b) are difference spectra, $\Delta A = A_p - A_u$, where A_p and A_u are the absorbances of the sample after and before the photoexcitation, respectively. The spectra have contributions from both excited-state absorption and ground-state bleach signal. Whereas the excited-state absorbance is positive and may evolve with time, the negative ground-state bleach signal is time-independent and identical to a scaled equilibrium absorbance of the sample. Any evolution of the excited-state absorption can be better viewed by eliminating the bleach component from the transient spectra through the addition of a scaled equilibrium absorption spectrum.^{15,35}

The scaling factor represents the fraction of the sample that is photoexcited and is the same for all time delays. Figure 3 shows the estimated time-dependent excited-state spectra after photoexcitation of CytCN in D_2O . By fitting the blue wing of the equilibrium spectrum to the 0.3-ps signal in the $2150 - 2130\text{ cm}^{-1}$ spectral range of the bleach signal (see Figure 1(b)), the smallest possible scaling factor that eliminates negative contribution from the transient spectra was determined to be 0.1. This method may result in an underestimated scaling factor with a relatively large error. The resulting spectra, arising from the molecules that have absorbed a 575 nm photon, show a small decaying absorption band at 2090 cm^{-1} (band 2) and a growing absorption band (band 1') that eventually becomes the CN fundamental of CytCN. The evolution of the excited-state absorption reflects the dynamics of the electronically and/or vibrationally excited

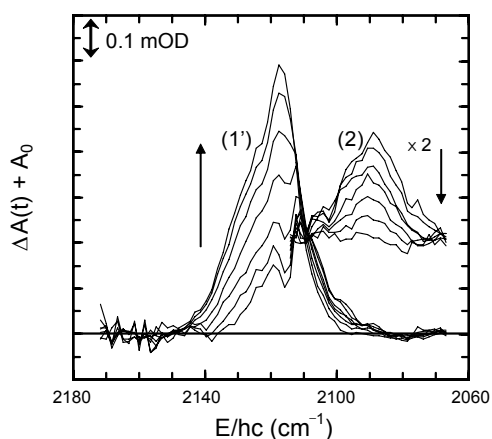


Figure 3. The transient absorption spectra after excitation with a pump pulse (A_p). They were obtained by adding the same scaled equilibrium CN absorption band to the time-resolved spectra ($\Delta A = A_p - A_u$), thus eliminating the bleach component, negative of the absorption spectrum before excitation ($-A_u$). For clarity, the quadratic background has been subtracted from the measured time-resolved spectra, two absorption features are separated, and band 2 is offset from band 1' and magnified two fold. The vertical arrows show the direction of the pump-probe delays in the order of 0.3, 0.56, 1, 1.8, 3.2, 5.6, and 10 ps.

molecule.

The evolution of band 1' shows the typical behavior of a vibrational band of a molecule cooling down (thermal relaxation).³⁶ Band 1' is initially broader and located at lower energies than the CN fundamental band. The decreasing frequency shift and narrowing band width reflect recovery of the equilibrium temperature of a molecule that initially had a larger vibrational temperature. Similar spectral evolution has been observed after photoexcitation of MbCN by 405-nm photon, where the spectral evolution of band 1' was attributed to heme cooling.¹⁵ The observed frequency shift of band 1' was thought to arise from the relaxation of the anharmonically coupled low-frequency modes that were excited during relaxation process of the photoexcited state. Here we also assigned band 1' to the CN fundamental band in an electronic ground state.¹⁵ Thus, the blue shift and the narrowing of band 1' arise from relaxation of the excited low-frequency modes anharmonically coupled to the CN fundamental. The evolution of band 1' can serve as a thermometer of the vibrational temperature of the molecule. The intensity of band 1' represents the number of CytcCN molecules that have relaxed to the vibrational ground state of the CN stretching in the electronic ground state. As the excited molecule returns to the electronic ground state and all the vibrational modes relax to the equilibrium state, the A_p spectrum becomes the same as the A_u spectrum, the equilibrium spectrum.

The time-dependent changes in the intensities and peak positions of the two bands are shown in Figure 4. Both the decay of band 2 and the growth of band 1' show an exponential dynamic with the same time constant of 1.9 ps. The two bands undergo a blue-shift with the same time constant of 2 ps, which is essentially identical to the time constant of intensity change (1.9 ps). Band 2 shifts 2.8 cm^{-1} and band 1' shifts almost twice as much as band 2 (6.1 cm^{-1}). As can be seen in Figure 4(a), the initial intensity of band 1' is about 40% of the full intensity, suggesting

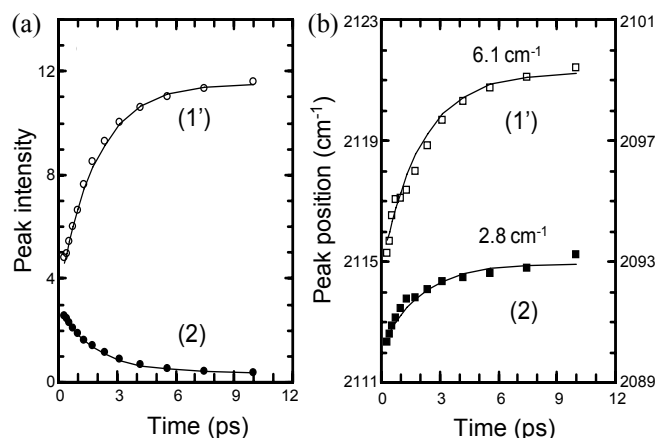


Figure 4. The time-dependent intensities (circles) and peak positions (squares) of bands 1' (open symbols) and 2 (filled symbols). They were well described by the exponential functions (the solid lines) with life times of 1.9 (intensities) and 2 ps (peak positions). Band 1' shifts 6.1 cm^{-1} starting from 2115 cm^{-1} at 0.3 ps and band 2 shifts 2.8 cm^{-1} from 2090 cm^{-1} .

that more than a third of the initially excited molecules are CN⁻ ligated and in the ground electronic state with the excited low-frequency modes. The full recovery of band 1' is synchronized with the decay of the band, implying that the population of the electronic ground state with the excited low-frequency modes is supplied by the state giving rise to band 2. Whereas growth of intensity represents growth of the population in the state, the shift of band 1' reveals a 2-ps vibrational cooling time for the heme in CytcCN. This is consistent with the value of 3.6 ps reported in MbCN¹⁵ and 3 ± 1 ps obtained by time-resolved anti-Stokes Raman spectroscopy after photolysis of MbCO.³⁷

Polarization-dependent spectra were obtained by setting the pump polarization parallel and perpendicular to the probe polarization. As shown in Figure 5, when spectra with a perpendicularly polarized pump and probe were multiplied by a factor of 1.2, they were completely superimposed on spectra with a parallel polarized pump and probe, showing that all the bands in the transient spectra have the same polarization anisotropy independent of the pump-probe delay. Non-decaying polarization anisotropy with time implies that the observed vibrational bands arise from the molecule with negligible rotational motion in 10 ps, the experimental time window here. The same anisotropy polarization for all bands indicates that these bands arise from the same molecule with different energy states or molecules with similar structures. The dissociated ligand, CN⁻, has much faster rotational time than the bulky CytcCN molecule and, thus, the anisotropy decay for the vibrational band of CN⁻ will be much faster than that of CytcCN. The same anisotropy change throughout the transient spectra suggests that band 2 cannot be assigned to the dissociated ligand. Instead, it likely arises from a ligand bound to the protein, CytcCN. The angle between the transition dipoles has been deduced from the polarization anisotropy of the sample. If the heme is a circular absorber at the pump wavelength, the angle between the CN transition dipole moment and the normal to the heme plane is determined to be 37° from the observed scale factor 1.2.³⁸ It is similar to the reported value of $30 \pm 8^\circ$ for MbCN,¹⁵ but is much larger

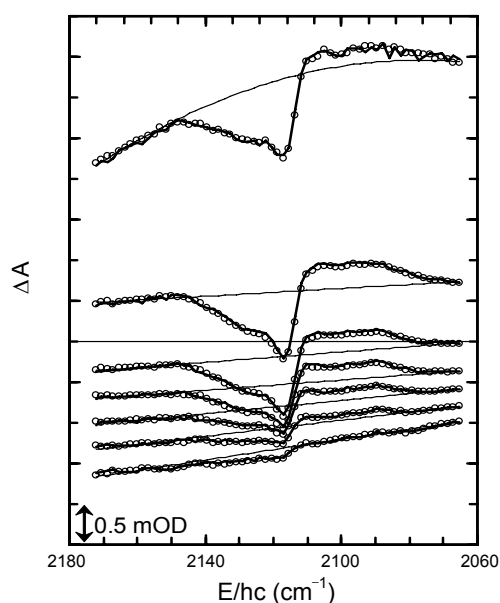


Figure 5. Representative time-resolved spectra for the pump polarization parallel with (open circles) and perpendicular to (the solid lines) probe polarization. Spectra for parallel polarization of pump and probe pulses were multiplied by a factor of 1.2 and shared the background of perpendicular polarization to superimpose signals from both polarizations. Pump-probe delays are 0.3, 0.56, 1, 1.8, 3.2, 5.6, and 10 ps from top to bottom.

than the value of 15° obtained from the equilibrium structure of Cyt_cCN in a solution determined by NMR.²³ The precise angle can be determined when the polarization anisotropy is measured in the limit of zero pump-induced change using perfect polarizers.³⁹⁻⁴¹ An imperfect polarizer and finite photoexcitation tend to underestimate the polarization anisotropy and thus overestimate the angle. The thermal motion of CN as well as the deviation of the heme planarity also contributes to the reduction of the polarization anisotropy. Therefore, the estimated angle from the polarization anisotropy is an upper limit.⁴⁰

As discussed above, the anisotropy measurement excludes the possibility that band 2 arises from the dissociated ligand. Since band 2 is 27 cm⁻¹ red-shifted from the CN fundamental mode that is very similar to the anharmonicity of the ¹³C¹⁵N⁻ stretching mode in D₂O, 26 cm⁻¹, it can be assigned to the hot CN stretching band of Cyt_cCN. However, the fast decay of band 2 requires an ultrafast vibrational relaxation time of < 1 ps.¹⁵ Furthermore, since band 2 is 3.3 times weaker than the bleach, only a fraction of the excited molecules are in a $v = 1$ state of the electronically ground state and about 77% of them are in IR-inactive state(s). The vibrational relaxation time from $v = 1$ to $v = 0$ in the CN⁻ in water was reported to be 28 - 120 ps.⁴² The vibrational relaxation time of the CN stretching mode in the heme bound CN has not been measured, but recent nonequilibrium MD simulation estimated that the relaxation time is hundreds of ps in MbCN.²⁶ Thus, it is unlikely that band 2 is a hot CN stretching band of Cyt_cCN. As suggested in MbCN, experimentally and theoretically,^{15,26} band 2 likely arises from CN stretching in the electronically excited state, where the CN bond is slightly weakened and its extinction coefficient is lowered.

Clearly, photo-deligation of Cyt_cCN by a 575-nm photon is highly inefficient. Inefficient photo-deligation of Cyt_cCN and MbCN suggests that ferric heme-bound CN⁻ is not photo-labile, which is a stark contrast to a ferrous heme-bound neutral ligand. Photolysis experiment on other anion-bound ferric hemes is under progress to determine whether inefficient photo-deligation is a general property of anion-bound ferric heme.

In conclusion, after Q-band excitation, photoexcited Cyt_cCN undergoes ultrafast radiationless relaxation without photo-deligation. The photoexcited molecule relaxes via an electronically excited state where the CN bond is weakened about 6% and its extinction coefficient is significantly lowered. As is the case in MbCN, photodissociation of CN⁻ from Cyt_cCN is also unlikely. Photo-inertness appears to be a general property of CN⁻-ligated ferric heme.

Acknowledgments. This research was supported by the Basic Science Research Program through the National Research Foundation of Korea (NRF), funded by the Ministry of Education, Science, and Technology (2010-0007469).

References

- Antonini, E.; Brunori, M. *Hemoglobin and Myoglobin in Their Reactions With Ligands*; North-Holland Publishing Company: London, UK, 1971.
- Austin, R. H.; Beeson, K. W.; Eisenstein, L.; Frauenfelder, H.; Gunsalus, I. C. *Biochemistry* **1975**, *14*, 5355.
- Kim, J.; Park, J.; Lee, T.; Lim, M. *J. Phys. Chem. B* **2009**, *113*, 260.
- Springer, B. A.; Sligar, S. G.; Olson, J. S.; Phillips, G. N., Jr. *Chem. Rev.* **1994**, *94*, 699.
- Ansari, A.; Berendzen, J.; Braundstein, D. K.; Cowen, B. R.; Frauenfelder, H.; Hong, M. K.; Iben, I. E. T.; Johnson, J. B.; Ormos, P.; Sauke, T. B.; Scholl, R.; Schulte, A.; Steinbach, P. J.; Vittitow, J.; Young, R. D. *Biophys. Chem.* **1987**, *26*, 337.
- Balasubramanian, S.; Lambright, D. G.; Marden, M. C.; Boxer, S. G. *Biochemistry* **1993**, *32*, 2202.
- Cornelius, P. A.; Steele, A. W.; Chernoff, D. A.; Hochstrasser, R. M. *Proc. Natl. Acad. Sci. USA* **1981**, *78*, 7526.
- Henry, E. R.; Sommer, J. H.; Hofrichter, J.; Eaton, W. A. *J. Mol. Biol.* **1983**, *166*, 443.
- Kim, S.; Jin, G.; Lim, M. *J. Phys. Chem. B* **2004**, *108*, 20366.
- Martin, J. L.; Migus, A.; Poyart, C.; Lecarpentier, Y.; Astier, R.; Antonetti, A. *Proc. Natl. Acad. Sci. USA* **1983**, *80*, 173.
- Petrich, J. W.; Lambry, J. C.; Kuczera, K.; Karplus, M.; Poyart, C.; Martin, J. L. *Biochemistry* **1991**, *30*, 3975.
- Walda, K. N.; Liu, X. Y.; Sharma, V. S.; Magde, D. *Biochemistry* **1994**, *33*, 2198.
- Ye, X.; Yu, A.; Champion, P. M. *J. Am. Chem. Soc.* **2006**, *128*, 1444.
- Ye, X.; Yu, A.; Georgiev, G. Y.; Gruia, F.; Ionascu, D.; Cao, W.; Sage, J. T.; Champion, P. M. *J. Am. Chem. Soc.* **2005**, *127*, 5854.
- Helbing, J.; Bonacina, L.; Pietri, R.; Bredenbeck, J.; Hamm, P.; van Mourik, F.; Chaussard, F. i.; Gonzalez-Gonzalez, A.; Chergui, M.; Ramos-Alvarez, C.; Ruiz, C.; Lopez-Garriga, J. *Biophys. J.* **2004**, *87*, 1881.
- Horecker, B. L.; Kornberg, A. *J. Biol. Chem.* **1946**, *165*, 11.
- George, P.; Tsou, C. L. *Biochem. J.* **1952**, *50*, 440.
- Petrich, J. W.; Poyart, C.; Martin, J. L. *Biochemistry* **1988**, *27*, 4049.
- Reddy, K. S.; Yonetani, T.; Tsuneshige, A.; Chance, B.; Kushkuley, B.; Stavrov, S. S.; Vanderkooi, J. M. *Biochemistry* **1996**, *35*, 5562.
- Boffi, A.; Chiancone, E.; Peterson, E. S.; Wang, J.; Rousseau, D.

- L.; Friedman, J. M. *Biochemistry* **1997**, *36*, 4510.
21. Negrerie, M.; Cianetti, S.; Vos Marten, H.; Martin, J.-L.; Kruglik Sergei, G. *J. Phys. Chem. B* **2006**, *110*, 12766.
22. Bolognesi, M.; Rosano, C.; Losso, R.; Borassi, A.; Rizzi, M.; Wittenberg, J. B.; Boffi, A.; Ascenzi, P. *Biophys. J.* **1999**, *77*, 1093.
23. Yao, Y.; Qian, C.; Ye, K.; Wang, J.; Bai, Z.; Tang, W. *J. Biol. Inorg. Chem.* **2002**, *7*, 539.
24. Varhac, R.; Antalík, M. *J. Biol. Inorg. Chem.* **2008**, *13*, 713.
25. Danielsson, J.; Meuwly, M. *ChemPhysChem* **2007**, *8*, 1077.
26. Danielsson, J.; Meuwly, M. *J. Phys. Chem. B* **2007**, *111*, 218.
27. Takano, T.; Kallai, O. B.; Swanson, R.; Dickerson, R. E. *J. Biol. Chem.* **1973**, *248*, 5234.
28. Sutin, N.; Yandell, J. K. *J. Biol. Chem.* **1972**, *247*, 6932.
29. Brautigan, D. L.; Feinberg, B. A.; Hoffman, B. M.; Margoliash, E.; Preisach, J.; Blumberg, W. E. *J. Biol. Chem.* **1977**, *252*, 574.
30. Morishima, I.; Inubushi, T. *FEBS Lett* **1977**, *81*, 57.
31. Lee, T.; Park, J.; Kim, J.; Joo, S.; Lim, M. *Bull. Korean Chem. Soc.* **2009**, *30*, 177.
32. Hamm, P.; Kaindl, R. A.; Stenger, J. *Opt. Lett.* **2000**, *25*, 1798.
33. Glasoe, P. K.; Long, F. A. *J. Phys. Chem.* **1960**, *64*, 188.
34. Yoshikawa, S.; O'Keeffe, D. H.; Caughey, W. S. *J. Biol. Chem.* **1985**, *260*, 3518.
35. Lim, M.; Jackson, T. A.; Anfinrud, P. A. *J. Phys. Chem.* **1996**, *100*, 12043.
36. Hamm, P.; Ohline, S. M.; Zinth, W. *J. Chem. Phys.* **1997**, *106*, 519.
37. Mizutani, Y.; Kitagawa, T. *Science* **1997**, *278*, 443.
38. Moore, J. N.; Hansen, P. A.; Hochstrasser, R. M. *Proc. Natl. Acad. Sci. USA* **1988**, *85*, 5062.
39. Ansari, A.; Szabo, A. *Biophys. J.* **1993**, *64*, 838.
40. Lim, M.; Jackson, T. A.; Anfinrud, P. A. *J. Am. Chem. Soc.* **2004**, *126*, 7946.
41. Locke, B.; Lian, T.; Hochstrasser, R. M. *Chem. Phys.* **1991**, *158*, 409.
42. Hamm, P.; Lim, M.; Hochstrasser, R. M. *J. Chem. Phys.* **1997**, *107*, 10523.
-